Free-standing film based on dissolution and homogeneous compounding of carbon nitride for photocatalytic sterilization

Xiaoxiao Peng[‡][a], Jin Ma[‡][a], Hong Yang[a], Kaiqing Wu[a], Zhixin Zhou[a], Qing Hong[a], Sicheng Liang[a], Songqin Liu[a], Yanfei Shen[b], Yuanjian Zhang[a]*

[a]Jiangsu Engineering Laboratory of Smart Carbon-Rich Materials and Device, Jiangsu Province Hi-Tech Key Laboratory for Bio-Medical Research, School of Chemistry and Chemical Engineering, Southeast University, Nanjing 211189, China, E-mail: Yuanjian.Zhang@seu.edu.cn

[b]Medical School, Southeast University, Nanjing 210009, China

Abstract

Polymeric carbon nitride (p-CN) has attracted increasing interest as a metal-free photocatalyst in energy conversion and bacterial disinfection. However, due to its particulate and insoluble nature, compounding p-CN at the molecular level into a functional composite of high performance remains a grand challenge. Here, we report the dissolution of p-CN in polyphosphoric acid (PPA) and the homogeneous compounding with carbon nanotubes (CNTs) into a free-standing film simply by co-dissolution, precipitation, and filtration. Interestingly, the as-prepared p-CN-CNTs film exhibited superior film strength than the pristine CNTs and nearly complete inactivation of *E. coli and S. aureus* under simulated solar irradiation with superoxide radicals as the dominant intermediates. Mechanistic studies indicated that the acidity and viscosity of PPA play crucial roles in the dissolution. The universality of this finding was supported by the further successful discovery of a new type of solvent for p-CN using task-specific ionic liquids. This work would provide a general way to address the dissolution difficulties of p-CN, and pave the prospective application of p-CN in nanocomposites at the molecular level.

Keywords: carbon nitride, dissolution, homogeneous compounding, free-standing film, photocatalytic sterilization

Introduction

Polymeric carbon nitride (p-CN) has widely emerged as a semiconductor-based photocatalyst in numerous interdisciplinary fields,[1-6] such as solar fuels, environmental remediation, and bacterial disinfection.[7, 8] The metal-free composition and photo-responsive specialty to visible light of p-CN can avoid secondary pollution,[9] caused by leaching metal ions and high energy consumption initiated by UV light source.[10-12] However, most applications of p-CN are in powder state[13, 14] or fixed on solid substrates.[15, 16] It is difficult so far to carry out the combination of p-CN with supplementary functional materials at molecular level, as the strong interlayer hydrogen bond and Van der Waals forces make it challenging to dissolve or disperse in common solvents.[17, 18] It is foreseeable that realizing the dissolution of CN would dramatically expand its application scope range considering the fact that the particulate properties and insoluble nature of p-CN set great limitation to the further developments.[19]

Despite several successful efforts of exfoliating and dispersing of CN,[20][21][22] there are still many drawbacks. [18, 23-26] For example, p-CN was dissolvable in concentrated sulfuric acid (H_2SO_4) or methyl sulfonic acid (MSA) to driver homogeneous photocatalytic conversion, luminescent poly(triazine imide) (PTI-LiBr)-based carbon nitride nanosheets were formed by spontaneous dissolution in polar aprotic solvents like dimethyl sulfoxide (DMSO), and special K, Na-poly(heptazine imide) (PHI)-based carbon nitride in water led to colloidal nanoparticles. However, these solvents were generally of strong oxidation and corrosion, or only appliable to specialized carbon nitrides, which impeded the popularization and scaling up.

Herein, we report the dissolution of p-CN in polyphosphoric acid (PPA), which is acidity and viscosity controllable, mild, and nonoxidizing. The generality was further verified by successful dissolution using task-specific ionic liquids that provide suitable acidity and viscosity. As PPA is also good solvents for disperse carbon nanotubes (CNTs), free-standing films, consisting of p-CN and CNTs, were prepared simply by co-dissolution, precipitation and filtration. Interestingly, the as-prepared p-CN-CNTs Film showed superior film strength than the pristine CNTs and remarkable sterilization

activity under visible light. This work would put forward new insights into the dissolution of p-CN, and greatly pave its prospective free-standing film applications at molecular level.

Results and discussion

Dissolution of p-CN in PPA.

In this study, p-CN was dissolved in polyphosphoric acid (PPA, 75%P_2O_5) to form a clear and transparent solution by heating and stirring (Figure 1a-b, S1). While PPA with other contents of P_2O_5 have different acidity and viscosity, resulting in different degrees of dissolution. The Tyndall phenomenon was due to the original PPA solvent itself, which stay unchanged after p-CN dissolved in PPA (Figure S2).

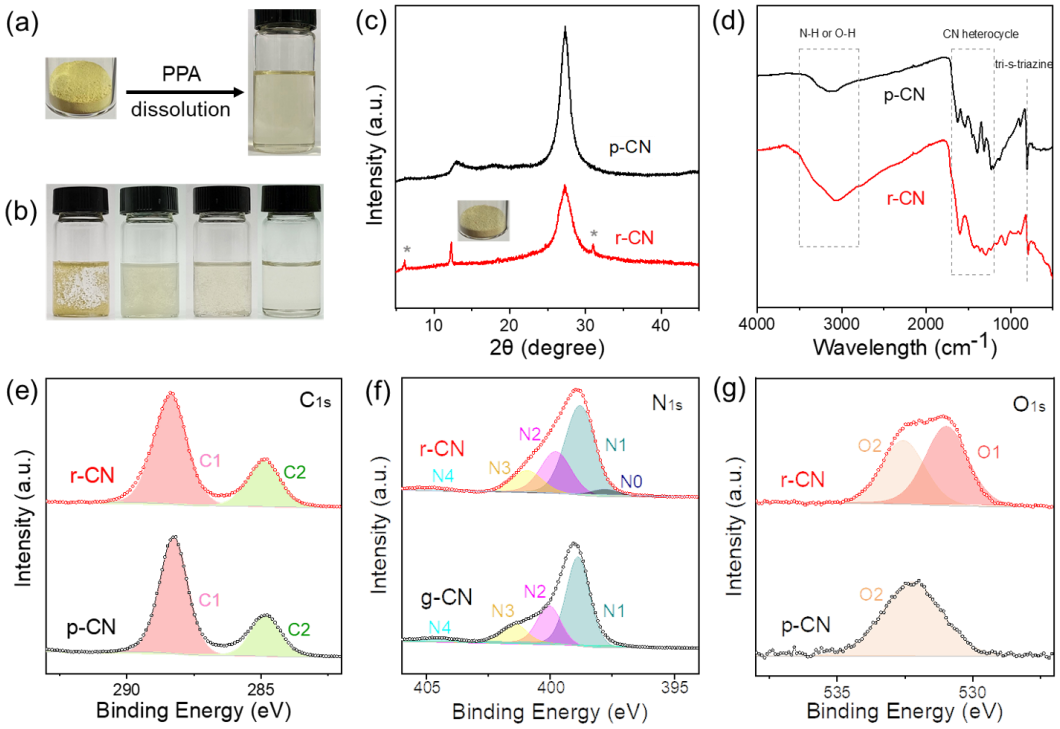

Figure 1. (a) Photograph of p-CN dissolved in PPA and (b) dissolving process. (c) XRD patterns of p-CN and r-CN. Inset: photograph of r-CN powder. (d) FT-IR spectra of p-CN and r-CN. XPS C_{1s} (e), N_{1s} (f) and O_{1s} (g) spectra of p-CN and r-CN.

As known, PPA almost has no oxidation activity. As such, the potential decomposition of p-CN in PPA could be avoided.[27] In order to evaluate whether the

structure of p-CN after the dissolution was changed or not, p-CN was precipitated using poor solvent methanol (CH_3OH). The recovered carbon nitride (denoted as r-CN) was still yellow (Figure 1c inset), consistent with the original color of p-CN; in contrast, smaller subunit of carbon nitrides are usually white. It indicated that p-CN was not decomposed during the dissolution. Notably, compared to pristine p-CN, the color and particle size of r-CN became lighter and smaller, respectively (Figure S3), which was ascribed to the protonation in PPA.[23, 24]

X-ray diffraction (XRD) illustrates r-CN retained two-dimensional layered structure for the conservation of identical 002 diffraction (Figure 1c, S4). The slight increase of peak width could be attributed to the disorder or expansion of the layered structure of p-CN caused by acid intercalation, and the decrease of peak intensity owing to the reduction of plane size and periodic interlayer stacking of CN layers. For both p-CN and r-CN, the characteristic Fourier transform infrared (FT-IR) spectra (Figure 1d) are mostly accordant as the peaks at 800 cm^{-1} (tri-s-triazine ring out of plane bending), 1200-1700 cm^{-1} (C-N aromatic heterocycle stretch vibration), 2800-3500 cm^{-1} (stretching vibration and hydrogen bond interaction) were retained. Some faint changes, such as the relative intensity of C-N heterocycle absorption peak or the shift of some characteristic peaks to low wavelength region, result from the protonation of acid.[28-30]

X-ray photoelectron spectroscopy (XPS) analysis was carried out to gain an in-depth understanding of the bonding properties. The C_{1s} XPS spectra (Figure 1e) display the same two obvious main peaks at 288.3 eV and 284.6 eV, belonging to N-C=N of carbon nitride and impurity carbon contamination,[31] respectively. Four N_{1s} peaks in Figure 1f correspond to N1 (-C=N-C, tri-s-triazine ring), N2 ($N-(C)_3$, bridging N atom), N3 (C-N-H, bonded with H atom) and N4 (charge effect) ,[32] the only difference is the extra peak (N0) of r-CN due to N-P bonding mode. In the O_{1s} spectra (Figure 1g), the existing O results in the adsorption of water, while the O content in r-CN were divided into PO_4^{3-} (O1) and H_2O (O2). P_{2p} spectra demonstrate the binding model of P (Figure S5), the two peaks could be attributed to the P-O and P-N bonds.[33, 34] To confirm the components, elemental analysis (Table S1) performed shows the approximate C/N mole

ratio before and after the dissolution. The increase of H mass fraction in r-CN, blue shift of UV absorbance and fluorescence spectra (FL) (Figure S6) were the evidences of protonation. Combing the results above, r-CN almost has no change compared with p-CN, the typical lamellar texture, electronic structure and chemical composition of p-CN were well maintained, revealed that p-CN is dissolved rather than decomposed in PPA.

Mechanism study of p-CN in dissolution.

In order to get a better understanding of the dissolution process and dissolution mechanism, the intermediate product p-CN-PPA paste (600 mg/mL) was prepared. As shown in Figure 2a-b, blue shift of UV absorption peak[27, 29] and the shift toward smaller 2θ values of XRD 002 peak indicated the part of solvent protonation and the possibility of intercalation. Another proof of the protonation came from the numerical value of zeta potential (Figure 2c), the zeta potential of CN dispersion in water shifted from negative to positive surface charges after contacting with PPA. Interestingly, p-CN could only be dissolved when the content of P_2O_5 is around 75%, as PPA with too much P_2O_5 is too sticky that fail to provide sufficient free H^+, and PPA with too less P_2O_5 is unfavorable for dispersion (Figure S7, S8). It was evident that viscous nature[35] which expressed in different P_2O_5 contents played a crucial part in the dissolution process (Figure 2d). Mechanical agitation needs to provide greater force for viscous liquid to flow. In a word, an appropriate viscosity (700 mPa·s in this paper) of the solvent provides strong shear force[36-38] on the surface of p-CN during mechanical stirring to boost dispersion and frustrate re-bundling, minimizing the structural damage to carbon materials during reaction, as well as making up for the less H^+ produced by its weaker acidity (Table S2) than strong acids and large density on the basis.

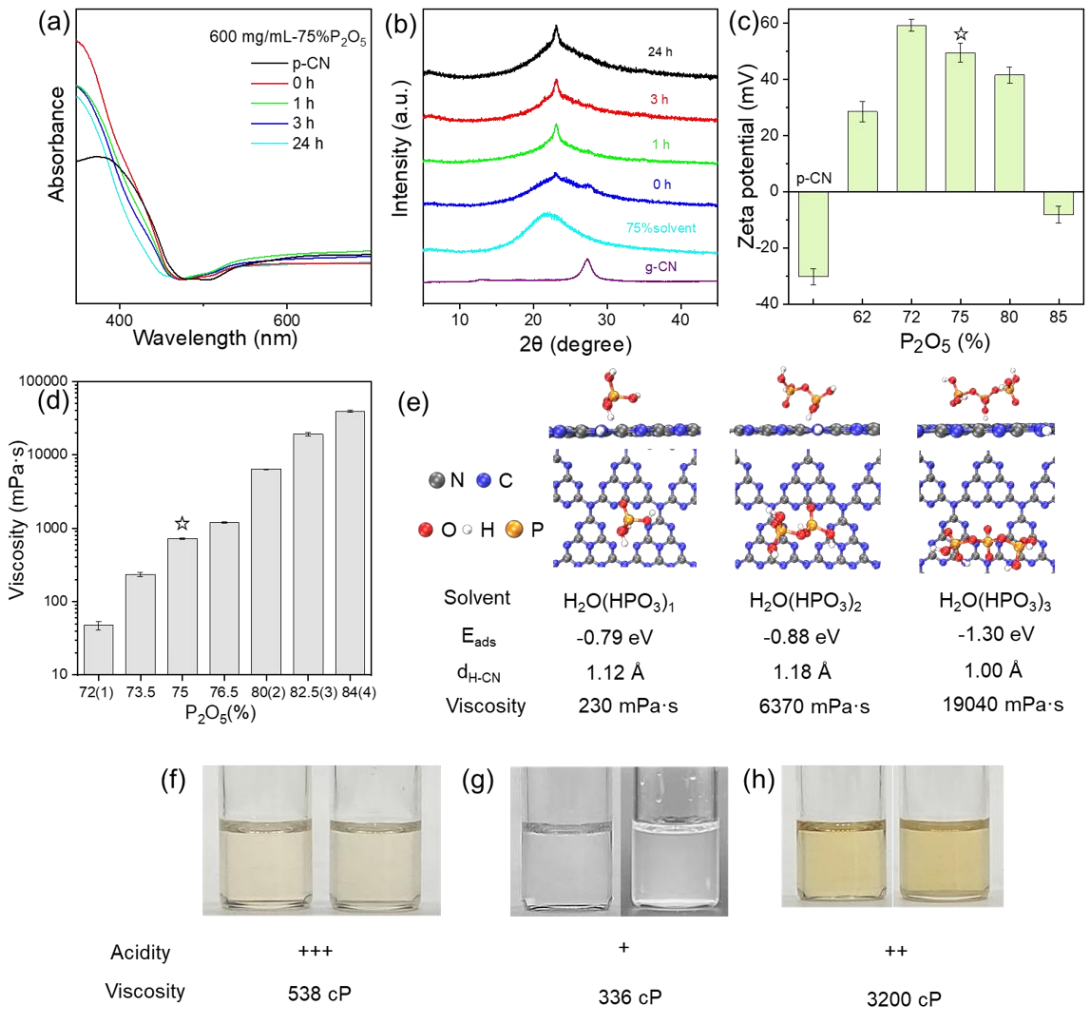

Figure 2. (a) Solid diffuse reflectance spectra of p-CN-PPA paste (600 mg/mL, 75%P_2O_5). (b) XRD patterns of p-CN-PPA paste (600 mg/mL, 75%P_2O_5). (c) Zeta potential of r-CN dispersions in water after precipitation from PPA with different P_2O_5 content. (d) Viscosity of PPA with different P_2O_5 content. The numbers in brackets on the abscissa axis represent the degree of polymerization of the corresponding acid. (e) Molecular models of mono-poly (P1), di-polyphosphoric acid (P2) and tri-polyphosphoric acid (P3). E_{ads} and $d_{H\text{-}CN}$ represent the adsorption energy and the distance between the nearest H atom and the plane structure of p-CN, respectively. Photographs of $C_{10}H_{14}F_3NO_6S_2$ (f), $C_8H_{15}F_6N_2P$ (g), $C_{12}H_{24}N_2O_4S$ (h).

Moreover, density functional theory (DFT) calculations were explored to prove dissolution.[39] (Figure S9). Generally speaking, the interaction between solvent molecules which possess strong adsorption capacity and carbon nitride has a greater

advantage for dissolution. The adsorption energy (E_{ads}) and the adsorption distance (d_{H-CN}) of mono-polyphosphoric acid (written simply as P1) and di-polyphosphoric acid (P2) (Figure 2e) were calculated as the solvent prepared in this paper is polyphosphoric acid with P_2O_5 content of 75% that between them. The calculated E_{ads} values for P1 (-0.79 eV) and P2 (-0.88 eV) were apparently higher than that for H_2O (-0.27 eV)[26], indicating PPA was a suitable solvent that dissolved p-CN remarkably faster and more effective than H_2O. The feasibility of dissolution was explained by DFT from thermodynamic point of view. However, tri-polyphosphoric acid (P3) exhibited stronger adsorption capacity (-1.30 eV) which could not dissolve p-CN in the experiments. The deviation between theoretical calculation and practical experiments showed that the binding mode and interaction of solvent molecules could not be ignored. From the dynamics, the relation between diffusion and viscosity is close,[40] the solute molecules diffuse through the solvent envelope in order to come into contact with other solvent molecules and react. According to Stokes-Einstein equation, viscosity is inversely proportional to diffusivity, which means that too much viscosity can hinder diffusion and molecular motion. In this regard, the appropriate viscosity of PPA promotes dispersion and compensates for the less H^+ produced by its weaker acidity. But viscosity is only an "auxiliary", when the degree of polymerization is too high and the viscosity is too big, it will take over the main.

Both viscosity and protonation are necessary to the successful dissolution of p-CN, and ionic liquids further support this conclusion (Figure 2f-h), as only the ionic liquids with proper viscosity and suitable proton acidity could dissolve CN better. Above all, the dissolution mechanism was summarized in Figure S10. The weak acidity of phosphoric acid protonates the surface protonation that lead to interlayer repulsion, PPA obtained from the mixture of mono/di-phosphoric acid is viscous and provides shear force to promote delamination under mechanical agitation, the cooperation of the two factors leads to p-CN dissolution.

Formation and structural characterization of composite CN-CNT-Film.

Figure 3a illustrates the fabrication process of CN-CNT-Film via a facile homogeneous compounding and filtration approach. Compared with various reported methods of CN-based film formation that were still far less than satisfactory (Table S3), this operation is obviously easy to synthesize, suitable for mass production and could be directly separated that no need for substrate. Firstly, mix p-CN and CNTs together to get a stable CN-CNT solution, then co-precipitate CN-CNT by CH_3OH through a constant pressure drop funnel to generate a uniform dispersion. Finally, the mixture was stably assembled into a composite film via π-π interaction by vacuum filtration. The thickness of the CN-CNT-Film could be easily regulated by changing the amount of starting materials.

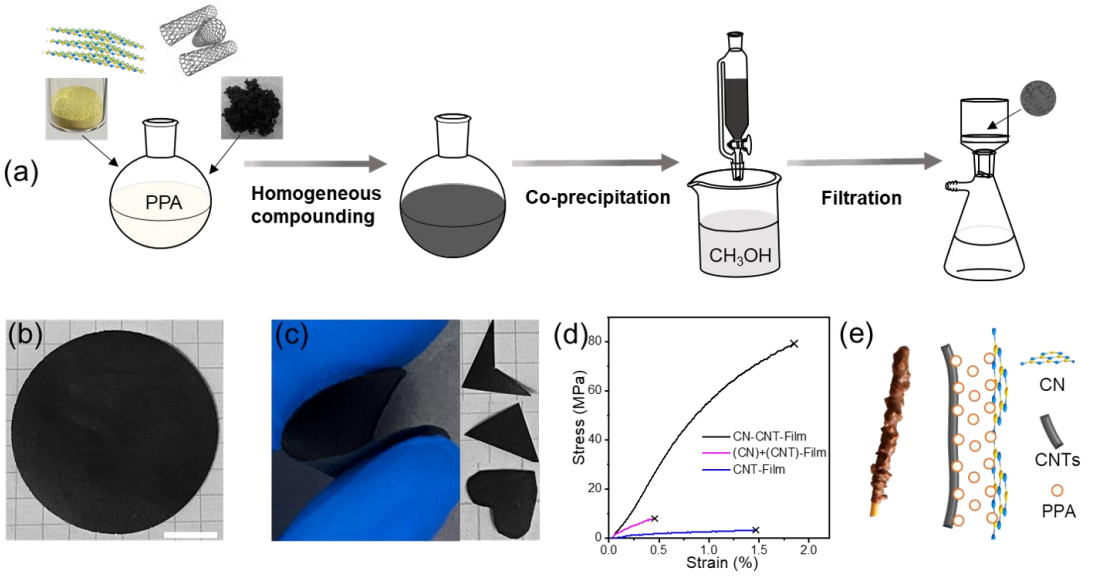

Figure 3. (a) Fabrication process of CN-CNT-Film. (b) Photo of the as-prepared CN-CNT-Film. Scale bar: 1 cm. (c) The free-standing CN-CNT-Film was 180° folded and cut into various shapes. (d) Stress-strain curves of CN-CNT-Film, (CN)+(CNT)-Film and CNT-Film. (e) Photograph of Pocky and the composite schematic diagram of CN and CNTs.

It is worth noting that, apart from being a good solvent (Figure 1a, S11),[38] PPA also plays a critical role in the process of material compounding and preparation of CN free-standing film. Contrast experiments were employed to support our view (Figure 3b, S12-16). Among all fabricated materials, CN-CNT-Film formed by homogeneous compounding in PPA and co-precipitation was the only one that could be expediently

peeled from the filtration membrane, exhibiting a flat and complete surface. From the morphologies results measured by scanning electron microscopy (SEM) images, CN and CNTs clung together, distributed evenly and densely. Besides, it displays good flexibility and excellent tailorable property, as it could be rolled up and cut into different shapes, no damage was observed even when an 180° bend was performed on it (Figure 3c). Elemental distribution in the CN-CNT-Film was revealed by EDS analysis (Figure S17-S19), the elements C, N and P were uniformly composited in the film, even selected a cluster for further observation from the transmission electron microscopy (TEM). In particular, we chose a part of the cross section, it could be seen that N and P penetrated into the interior, manifesting that the compound did not simply stay on the surface. Tensile test was conducted to evaluate the mechanical properties (Figure 3d, S20), the results show that the ultimate strength and Young's modulus of CN-CNT-Film are obviously better than the others, indicating PPA definitely not to be neglected in the compounding, and the addition of CN contributed significantly to improve the mechanical properties of CNT-Film. This is similar to the structure of Pocky, a chocolate chip cookie bar with nuts, indeed, CN, CNTs and PPA were like nuts, cookie bar and chocolate, respectively (Figure 3e). Additionally, FT-IR spectra, Raman spectroscopy and XRD patterns of the film were carried out to prove the successful recombination of CN and CNTs (Figure S21).

Antibacterial performance of CN-CNT-Film.

The metal-free catalyst CN with visible light response has been used repeatedly in environmental remediation and disinfection. Unfortunately, almost all bacteria are negatively charged so that they have poor contact with the negatively charged p-CN. Meanwhile, the specific surface area of CN powder is small and it is difficult to recycle, makes it ineffective and inefficiency in bacteriostasis. Antibacterial performance of CN materials was improved by CN-CNT-Film that is positively charged (Figure S22) with more active sites. *E. coli* and *S. aureus* were used as the bacteria sources to support the results, as the photographs shown in Figure 4a-b, the antibacterial performance of CN-

CNT-Film was remarkable under visible light illumination. The photocatalytic disinfection efficiency for *E. coli* and *S. aureus* (10^9 CFU/mL) reached more than 99.9% within 2 hours, and the bacteria hardly regrow after photocatalysis (Figure S23-24). This performance is superior to the original p-CN and it is comparable with previously reported metal modified and heterostructured CN (Table S4). Furthermore, after it has been continuously used for several times (Figure S25), CN-CNT-Film still keeps sufficient activity, revealing that it is suitable for repeated and long-term use.

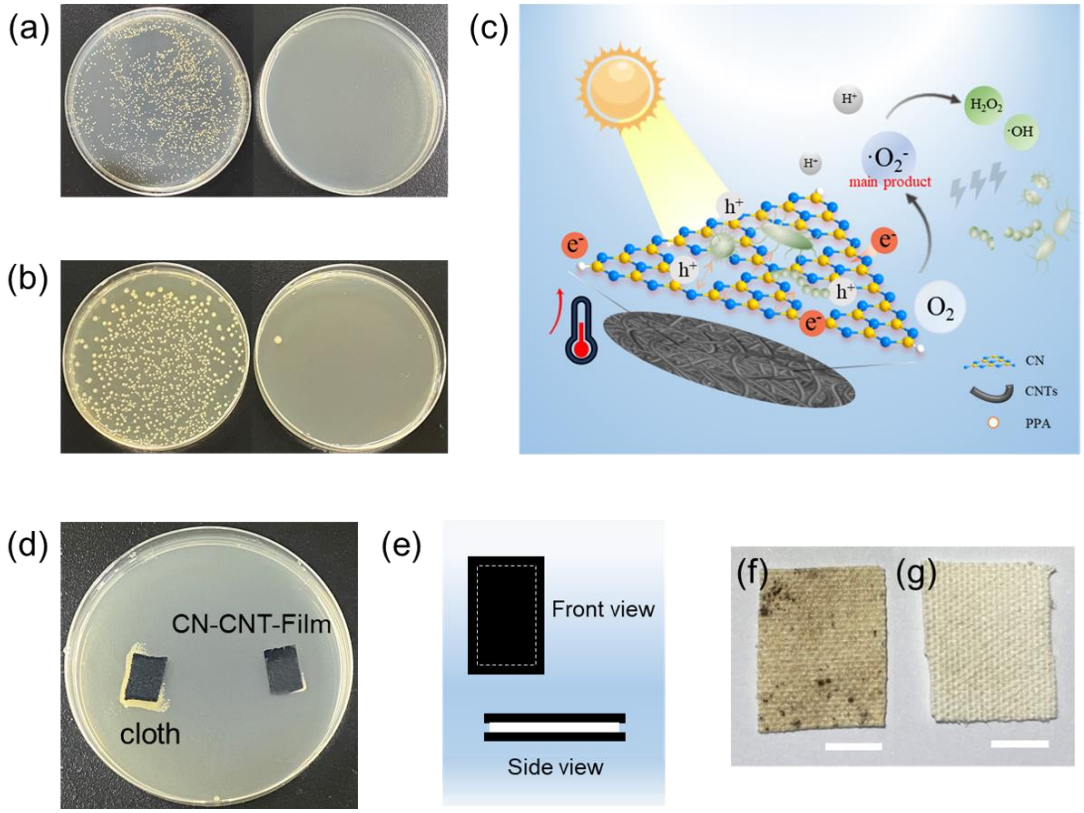

Figure 4. Photographs of bacterial colonies of *S. aureus* (a) and *E. coli* (b) before and after incubating with CN-CNT-Film under visible light. (c) Photocatalytic sterilization schematic of CN-CNT-Film. (d) Antibacterial effect comparison of normal cloth and CN-CNT-Film. (e) Schematic diagram of sandwich structure in simulation experiments. The growth of bacteria on the white cloth between clothes (f) and CN-CNT-Films (g).

Figure 4c demonstrated the mechanism of photocatalytic sterilization, CN-CNT-Film produced reactive oxygen species (ROS), the activation of O_2 by reduction via photogenerated electrons into $\bullet O_2^-$ was the major step (Figure S29-32), directly

sterilized under visible light, cooperating with suitable adsorption and faint photothermal effect (Figure S26-28). [41] As a proof of concept, we also displayed the potential application of CN-CNT-Film in disinfecting and protective equipment. As shown in Figure 4d-g, two layers of normal cloth or CN-CNT-Film and a piece of white cloth formed in sandwich structure in the same size were soaked in sewage with *S. aureus*, then illuminated them under the sunlight intermittently, the white cloth between the clothes grew bacteria in natural environment, while CN-CNT-Film as antibacterial material has no bacteria growing out under sunlight as the it suppressed the growth of bacteria, and inhibition zone experiment showed the same result. Therefore, CN-CNT-Film might have practical applications in smart sterilization garments for the wild and textile industry. In addition, it is believed that the film has a huge development prospect for making specific devices, such as filter or fish tank (Figure S33-34), to sterilization or water purification.

Conclusion

In summary, p-CN was successfully dissolved in a new generation solvent (PPA), and p-CN and CNTS were successfully composited into a free-standing film, simply by co-dissolution, precipitation and filtration. The prepared p-CN-CNT film achieved non-powder application of p-CN with greatly enhanced mechanical properties and showed an excellent photocatalytic sterilization activity. Notably, PPA is mild, playing an important role in the compound process. Mechanistic studies indicated that the acidity and viscosity of PPA play crucial roles in the dissolution. The universality of this finding was supported by further successful discovery of new type of solvents for p-CN using task-specific ionic liquids. This study provides a new path to understand the interactions at the molecular level, valuable insights for non-metal photocatalytic antibacterial film materials, and also a promising prospective for the design of actual sterilization and purification instruments going into practice.

References

1. Lv, Y.; Chen, S.; Shen, Y.; Ji, J.; Zhou, Q.; Liu, S.; Zhang, Y., Competitive Multiple-Mechanism-Driven Electrochemiluminescent Detection of 8-Hydroxy-2′-deoxyguanosine. *Journal of the American Chemical Society* **2018,** *140* (8), 2801-2804.

2. Zhao, T.; Zhou, Q.; Lv, Y.; Han, D.; Wu, K.; Zhao, L.; Shen, Y.; Liu, S.; Zhang, Y., Ultrafast Condensation of Carbon Nitride on Electrodes with Exceptional Boosted Photocurrent and Electrochemiluminescence. *Angewandte Chemie International Edition* **2019,** *59* (3), 1139-1143.

3. Podjaski, F.; Lotsch, B. V., Optoelectronics Meets Optoionics: Light Storing Carbon Nitrides and Beyond. *Advanced Energy Materials* **2020,** *11* (4).

4. Li, J.; Zhang, K.; Zhao, Y.; Wang, C.; Wang, L.; Wang, L.; Liao, M.; Ye, L.; Zhang, Y.; Gao, Y.; Wang, B.; Peng, H., High-Efficiency and Stable Li−CO2 Battery Enabled by Carbon Nanotube/Carbon Nitride Heterostructured Photocathode. *Angewandte Chemie International Edition* **2021,** *61* (4).

5. Kessler, F. K.; Zheng, Y.; Schwarz, D.; Merschjann, C.; Schnick, W.; Wang, X.; Bojdys, M. J., Functional carbon nitride materials — design strategies for electrochemical devices. *Nature Reviews Materials* **2017,** *2* (6).

6. Zhou, Z.; Zhang, Y.; Shen, Y.; Liu, S.; Zhang, Y., Molecular engineering of polymeric carbon nitride: advancing applications from photocatalysis to biosensing and more. *Chemical Society Reviews* **2018,** *47* (7), 2298-2321.

7. Teng, Z.; Yang, N.; Lv, H.; Wang, S.; Hu, M.; Wang, C.; Wang, D.; Wang, G., Edge-Functionalized g-C3N4 Nanosheets as a Highly Efficient Metal-free Photocatalyst for Safe Drinking Water. *Chem* **2019,** *5* (3), 664-680.

8. Ong, W.-J.; Tan, L.-L.; Ng, Y. H.; Yong, S.-T.; Chai, S.-P., Graphitic Carbon Nitride (g-C3N4)-Based Photocatalysts for Artificial Photosynthesis and Environmental Remediation: Are We a Step Closer To Achieving Sustainability? *Chemical Reviews* **2016,** *116* (12), 7159-7329.

9. Li, P.; Li, J.; Feng, X.; Li, J.; Hao, Y.; Zhang, J.; Wang, H.; Yin, A.; Zhou, J.; Ma, X.; Wang, B., Metal-organic frameworks with photocatalytic bactericidal activity for integrated air cleaning. *Nature Communications* **2019,** *10* (1).

10. Zeng, X.; Liu, Y.; Xia, Y.; Uddin, M. H.; Xia, D.; McCarthy, D. T.; Deletic, A.; Yu, J.; Zhang, X., Cooperatively modulating reactive oxygen species generation and bacteria-photocatalyst contact over graphitic carbon nitride by polyethylenimine for rapid water disinfection. *Applied Catalysis B: Environmental* **2020,** *274*.

11. Xia, P.; Cao, S.; Zhu, B.; Liu, M.; Shi, M.; Yu, J.; Zhang, Y., Designing a 0D/2D S-Scheme Heterojunction over Polymeric Carbon Nitride for Visible-Light Photocatalytic Inactivation of Bacteria. *Angewandte Chemie International Edition* **2020,** *59* (13), 5218-5225.

12. Wang, T.; Bai, Z.; Wei, W.; Hou, F.; Guo, W.; Wei, A., β-Cyclodextrin-Derivative-Functionalized Graphene Oxide/Graphitic Carbon Nitride Composites with a Synergistic Effect for Rapid and Efficient Sterilization. *ACS Applied Materials & Interfaces* **2022,** *14* (1), 474-483.

13. Zhou, M.; Ou, H.; Li, S.; Qin, X.; Fang, Y.; Lee, S. c.; Wang, X.; Ho, W., Photocatalytic Air Purification Using Functional Polymeric Carbon Nitrides. *Advanced Science* **2021,** *8* (24).

14. Ma, X.; Cheng, H., Synergy of nitrogen vacancies and intercalation of carbon species for enhancing sunlight photocatalytic hydrogen production of carbon nitride. *Applied Catalysis B: Environmental* **2022,** *314*.

15. Shalom, M.; Gimenez, S.; Schipper, F.; Herraiz-Cardona, I.; Bisquert, J.; Antonietti, M.,

Controlled Carbon Nitride Growth on Surfaces for Hydrogen Evolution Electrodes. *Angewandte Chemie International Edition* **2014,** *53* (14), 3654-3658.

16. Mazzanti, S.; Manfredi, G.; Barker, A. J.; Antonietti, M.; Savateev, A.; Giusto, P., Carbon Nitride Thin Films as All-In-One Technology for Photocatalysis. *ACS Catalysis* **2021,** *11* (17), 11109-11116.

17. Xu, J.; Antonietti, M., The Performance of Nanoparticulate Graphitic Carbon Nitride as an Amphiphile. *Journal of the American Chemical Society* **2017,** *139* (17), 6026-6029.

18. Krivtsov, I.; Mitoraj, D.; Adler, C.; Ilkaeva, M.; Sardo, M.; Mafra, L.; Neumann, C.; Turchanin, A.; Li, C.; Dietzek, B.; Leiter, R.; Biskupek, J.; Kaiser, U.; Im, C.; Kirchhoff, B.; Jacob, T.; Beranek, R., Water-Soluble Polymeric Carbon Nitride Colloidal Nanoparticles for Highly Selective Quasi-Homogeneous Photocatalysis. *Angewandte Chemie* **2019,** *132* (1), 495-503.

19. Jia, C.; Yang, L.; Zhang, Y.; Zhang, X.; Xiao, K.; Xu, J.; Liu, J., Graphitic Carbon Nitride Films: Emerging Paradigm for Versatile Applications. *ACS Applied Materials & Interfaces* **2020,** *12* (48), 53571-53591.

20. Yang, S.; Gong, Y.; Zhang, J.; Zhan, L.; Ma, L.; Fang, Z.; Vajtai, R.; Wang, X.; Ajayan, P. M., Exfoliated Graphitic Carbon Nitride Nanosheets as Efficient Catalysts for Hydrogen Evolution Under Visible Light. *Advanced Materials* **2013,** *25* (17), 2452-2456.

21. Lou, S.; Zhou, Z.; Shen, Y.; Zhan, Z.; Wang, J.; Liu, S.; Zhang, Y., Comparison Study of the Photoelectrochemical Activity of Carbon Nitride with Different Photoelectrode Configurations. *ACS Applied Materials & Interfaces* **2016,** *8* (34), 22287-22294.

22. Hu, P.; Chen, C.; Zeng, R.; Xiang, J.; Huang, Y.; Hou, D.; Li, Q.; Huang, Y., Facile synthesis of bimodal porous graphitic carbon nitride nanosheets as efficient photocatalysts for hydrogen evolution. *Nano Energy* **2018,** *50*, 376-382.

23. Zhou, Z.; Wang, J.; Yu, J.; Shen, Y.; Li, Y.; Liu, A.; Liu, S.; Zhang, Y., Dissolution and Liquid Crystals Phase of 2D Polymeric Carbon Nitride. *Journal of the American Chemical Society* **2015,** *137* (6), 2179-2182.

24. Zhang, J.; Zhang, M.; Lin, L.; Wang, X., Sol Processing of Conjugated Carbon Nitride Powders for Thin-Film Fabrication. *Angewandte Chemie* **2015,** *127* (21), 6395-6399.

25. Miller, T. S.; Suter, T. M.; Telford, A. M.; Picco, L.; Payton, O. D.; Russell-Pavier, F.; Cullen, P. L.; Sella, A.; Shaffer, M. S. P.; Nelson, J.; Tileli, V.; McMillan, P. F.; Howard, C. A., Single Crystal, Luminescent Carbon Nitride Nanosheets Formed by Spontaneous Dissolution. *Nano Letters* **2017,** *17* (10), 5891-5896.

26. Huang, C.; Wen, J.; Shen, Y.; He, F.; Mi, L.; Gan, Z.; Ma, J.; Liu, S.; Ma, H.; Zhang, Y., Dissolution and homogeneous photocatalysis of polymeric carbon nitride. *Chemical Science* **2018,** *9* (41), 7912-7915.

27. Zhang, Y.; Antonietti, M., Photocurrent Generation by Polymeric Carbon Nitride Solids: An Initial Step towards a Novel Photovoltaic System. *Chemistry - An Asian Journal* **2010,** *5*.

28. Jürgens, B.; Irran, E.; Senker, J.; Kroll, P.; Müller, H.; Schnick, W., Melem (2,5,8-Triamino-tri-s-triazine), an Important Intermediate during Condensation of Melamine Rings to Graphitic Carbon Nitride: Synthesis, Structure Determination by X-ray Powder Diffractometry, Solid-State NMR, and Theoretical Studies. *Journal of the American Chemical Society* **2003,** *125* (34), 10288-10300.

29. Zhang, Y.; Thomas, A.; Antonietti, M.; Wang, X., Activation of Carbon Nitride Solids by Protonation: Morphology Changes, Enhanced Ionic Conductivity, and Photoconduction Experiments. *Journal of the American Chemical Society* **2008,** *131* (1), 50-51.

30. Zhang, X.; Xie, X.; Wang, H.; Zhang, J.; Pan, B.; Xie, Y., Enhanced Photoresponsive Ultrathin Graphitic-Phase C3N4 Nanosheets for Bioimaging. *Journal of the American Chemical Society* **2012,** *135* (1), 18-21.
31. Lin, Z.; Wang, X., Nanostructure Engineering and Doping of Conjugated Carbon Nitride Semiconductors for Hydrogen Photosynthesis. *Angewandte Chemie International Edition* **2013,** *52* (6), 1735-1738.
32. Wu, W.; Zhang, J.; Fan, W.; Li, Z.; Wang, L.; Li, X.; Wang, Y.; Wang, R.; Zheng, J.; Wu, M.; Zeng, H., Remedying Defects in Carbon Nitride To Improve both Photooxidation and H2 Generation Efficiencies. *ACS Catalysis* **2016,** *6* (5), 3365-3371.
33. Wu, J.; Yang, S.; Li, J.; Yang, Y.; Wang, G.; Bu, X.; He, P.; Sun, J.; Yang, J.; Deng, Y.; Ding, G.; Xie, X., Electron Injection of Phosphorus Doped g-C3N4Quantum Dots: Controllable Photoluminescence Emission Wavelength in the Whole Visible Light Range with High Quantum Yield. *Advanced Optical Materials* **2016,** *4* (12), 2095-2101.
34. Chen, C.; Sun, X.; Yan, X.; Wu, Y.; Liu, H.; Zhu, Q.; Bediako, B. B. A.; Han, B., Boosting CO2 Electroreduction on N,P-Co-doped Carbon Aerogels. *Angewandte Chemie International Edition* **2020,** *59* (27), 11123-11129.
35. Baek, J.-B.; Lyons, C. B.; Tan, L.-S., Grafting of Vapor-Grown Carbon Nanofibers via in-Situ Polycondensation of 3-Phenoxybenzoic Acid in Poly(phosphoric acid). *Macromolecules* **2004,** *37* (22), 8278-8285.
36. Han, S.-W.; Oh, S.-J.; Tan, L.-S.; Baek, J.-B., One-pot purification and functionalization of single-walled carbon nanotubes in less-corrosive poly(phosphoric acid). *Carbon* **2008,** *46* (14), 1841-1849.
37. Yue, D.-C.; Ma, T.-B.; Hu, Y.-Z.; Yeon, J.; van Duin, A. C. T.; Wang, H.; Luo, J., Tribochemistry of Phosphoric Acid Sheared between Quartz Surfaces: A Reactive Molecular Dynamics Study. *The Journal of Physical Chemistry C* **2013,** *117* (48), 25604-25614.
38. Seo, J.-M.; Tan, L.-S.; Baek, J.-B., Defect/Edge-Selective Functionalization of Carbon Materials by “Direct” Friedel-Crafts Acylation Reaction. *Advanced Materials* **2017,** *29* (19).
39. Zhu, B.; Zhang, L.; Cheng, B.; Yu, J., First-principle calculation study of tri-s-triazine-based g-C3N4: A review. *Applied Catalysis B: Environmental* **2018,** *224*, 983-999.
40. Hiss, T. G.; Cussler, E. L., Diffusion in high viscosity liquids. *AIChE Journal* **1973,** *19* (4), 698-703.
41. Song, C.; Wang, Z.; Yin, Z.; Xiao, D.; Ma, D., Principles and applications of photothermal catalysis. *Chem Catalysis* **2022,** *2* (1), 52-83.